1
Inter-electron Repulsion and Irregularities in the Chemistry of Transition Series

David A. Johnson

1.1
Introduction: Irregularities in Lanthanide Chemistry

Both ligand field effects and inter-electronic repulsion produce irregularities in the chemistry of transition series. Irregularities due to inter-electronic repulsion are most obvious in the lanthanide series where ligand field effects are very small. For the first century of lanthanide chemistry, talk of irregularities would have seemed ridiculous. The laborious discovery and separation of the elements by the classical techniques of fractional crystallization and precipitation naturally led to the view that the lanthanides were all very much alike. But by 1933, Klemm had exposed inadequacies in this similarity paradigm when he made dihalides of samarium, europium and ytterbium by hydrogen reduction and thermal decomposition of trihalides [1, 2]. The compounds had crystal structures that were also to be found among the alkaline earth dihalides. On an ionic formulation, they contain Ln^{2+} ions with the configurations $[Xe]4f^6$, $[Xe]4f^7$ and $[Xe]4f^{14}$.

Klemm's work revealed important differences among some of the rare earth elements. But their full extent was made apparent by Corbett and his coworkers [2, 3a]. Corbett devised techniques for the determination of Ln/LnX_3 phase diagrams in tantalum and molybdenum containers in the temperature range 500–1200 °C. This use of more powerful reducing agents led to the preparation of alkaline earth-like dihalides of neodymium, dysprosium and thulium. Moreover, the conditions that generated new dihalides for some lanthanide elements failed to do so for others. For example, Corbett's work suggested that, whereas dihalides of dysprosium [4, 5] and thulium [6] were stable to disproportionation, those of erbium [7] were not. This was especially interesting because Klemm had emphasized that in both halves of the lanthanide series, this stability of the +2 oxidation state increased: in the first half up to the half-filled shell configuration at europium and in the second up to the filled shell at ytterbium [1]. The instability of erbium dihalides showed that in the second half of the series this increase was broken. Indeed, by combining a survey of the success or failure of preparative attempts with metal solubilities in molten trichlorides, it was possi-

Inorganic Chemistry in Focus III.
Edited by G. Meyer, D. Naumann, L. Wesemann
Copyright © 2006 WILEY-VCH Verlag GmbH & Co. KGaA, Weinheim
ISBN: 3-527-31510-1

ble to compile a stability sequence for the dipositive state across the entire series: La < Ce < Pr < Nd < (Pm) < Sm < Eu ≫ Gd < Tb < Dy > Ho > Er < Tm < Yb [2]. Stoichiometric alkaline earth-like dihalides are known only for Nd, Sm, Eu, Dy, Tm and Yb, although those of Pm could almost certainly be obtained if desired (I exclude metallic diiodides, e.g., LaI_2). The neodymium, thulium and dysprosium dihalides are exceptionally powerful reducing agents and may therefore have synthetic applications. For instance, in the presence of amide or aryloxide ligands, the di-iodides dissolve in THF and reduce nitrogen gas. The reduced di-nitrogen bridges two lanthanide(III) sites in a μ-η^2: η^2-N_2^{2-} arrangement [8].

The stability sequence given above applies to both of the following situations:

$$MCl_2(s) + 1/2\,Cl_2(g) = MCl_3(s) \tag{1}$$

$$MCl_2(s) = 1/3\,M(s) + 2/3\,MCl_3(s) \tag{2}$$

How can it be explained? It is useful to begin with reaction (1). By constructing a thermodynamic cycle around this reaction, we obtain the equation,

$$\Delta G^0(1) = I_3 + L(MCl_3, s) - L(MCl_2, s) + C \tag{3}$$

Here I_3 is the third ionization enthalpy of the lanthanide element and $L(MCl_n,s)$ is ΔH^0 for the following reaction:

$$M^{n+}(g) + nCl^-(g) = MCl_n(s) \tag{4}$$

The term C, which includes the enthalpy of formation of the gaseous chloride ion and $-T\Delta S^0(1)$, varies very little across the series. Thus the variations in $\Delta G^0(1)$ are determined by those in the first three terms on the right of Eq. (3). The combination of smooth lanthanide contractions with negligible ligand field effects suggests that $[L(MCl_3,s)–L(MCl_2,s)]$ should change smoothly and slightly across the lanthanide series. Consequently the variations in $\Delta G^0(1)$ should be almost entirely determined by those in I_3.

When this analysis was first attempted [9–11] very few values of I_3 had been obtained from series limits in the third spectra of the lanthanides, and the first comprehensive sets were calculated from Born-Haber cycles [9]. Subsequent spectroscopic values [12] confirmed the early work and are plotted in Fig. 1.1. In all cases they refer to the ionization process

$$M^{2+}([Xe]4f^{n+1}, g) = M^{3+}([Xe]4f^n, g) + e^-(g) \tag{5}$$

The specified configurations are ground-state configurations except at $La^{2+}(g)$ and $Gd^{2+}(g)$ where the ground states are $[Xe]5d^1$ and $[Xe]4f^75d^1$ respectively. It can be seen that the variations in I_3 do indeed correspond to the stability sequence for the dipositive oxidation state. The correspondence can also be tested quantitatively by using estimated and experimental values of $\Delta G^0(1)$. These are also plotted in Fig. 1.1. The parallelism between the two is very close.

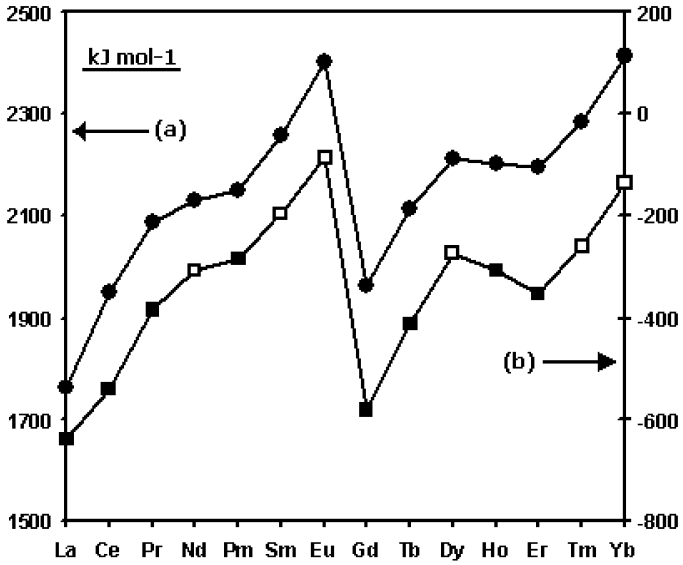

Fig. 1.1 (a) The ionization enthalpies of dipositive lanthanide ions with configurations of the type $[Xe]4f^{n+1}$ (upper plot; left-hand axis). (b) The standard Gibbs energy change of reaction 1 (lower plot; right-hand axis; ■ estimated value; □ experimental value). Data are from Refs. [11–14].

Figure 1.1 shows that the stability sequence revealed by chemical reactions and chemical synthesis *corresponds* to thermodynamic stabilities. An *explanation* requires a theory that will explain both. To get it we apply the theory of atomic spectra [9]. The energy of the 4f electrons in an ion with the configuration $[Xe]4f^n$, $E(4f^n)$, can be written $[nU+E_{rep}(4f^n)]$ where U, a negative quantity, is the energy of each 4f electron in the field of the positively charged xenon core, and $E_{rep}(4f^n)$ represents the repulsion between the n 4f electrons. In Table 1.1, $E_{rep}(4f^n)$ is expressed as a function of the Racah parameters E^0, E^1 and E^3. The subsequent column gives the ionization energy of each configuration, $[E(f^{n-1})-E(f^n)]$.

Despite our neglect of spin-orbit coupling, the theoretical ionization energies of columns 3 and 6 account for the I_3 variation in Fig. 1.1. The term $[-U-(n-1)E^0]$ leads to an overall increase across the series brought about by the increasing nuclear charge. But this increase is set back after the half-filled shell by the appearance of the quantity $-9E^1$. Finally the terms in E^3 produce irregularities in the 1/4- and 3/4-shell regions. Because the Racah parameters increase steadily across the series as the f-orbitals contract and inter-electronic repulsion rises, E^3 is greater in the second half of the series than in the first. Indeed, the terms in E^3 are then large enough to eliminate the overall increase in ionization energy between f^{10} and f^{12}, so dysprosium(II) compounds are more stable than those of erbium(II).

Table 1.1 The inter-electronic repulsion energies, $E_{rep}(f^n)$, and the ionization energies, $I(f^n)$, of f^n configurations according to the theory of atomic spectra.

n	$E_{rep}(f^n)$	$I(f^n)$	n	$E_{rep}(f^n)$	$I(f^n)$
0	0				
1	0	$-U$	8	$28E^0+9E^1$	$-U-7E^0-9E^1$
2	E^0-9E^3	$-U-E^0+9E^3$	9	$36E^0+18E^1-9E^3$	$-U-8E^0-9E^1+9E^3$
3	$3E^0-21E^3$	$-U-2E^0+12E^3$	10	$45E^0+27E^1-21E^3$	$-U-9E^0-9E^1+12E^3$
4	$6E^0-21E^3$	$-U-3E^0$	11	$55E^0+36E^1-21E^3$	$-U-10E^0-9E^1$
5	$10E^0-9E^3$	$-U-4E^0-12E^3$	12	$66E^0+45E^1-9E^3$	$-U-11E^0-9E^1-12E^3$
6	$15E^0$	$-U-5E^0-9E^3$	13	$78E^0+54E^1$	$-U-12E^0-9E^1-9E^3$
7	$21E^0$	$-U-6E^0$	14	$91E^0+63E^1$	$-U-13E^0-9E^1$

The *mathematics* of the theory of Table 1.1 therefore accounts for the variations in both I_3 and in the stability of alkaline earth-like dihalides. There remains the question of a *physical* explanation. The most important irregularity is the very large downward break after the half-filled shell, and the main contribution to it comes from the exchange energy [15]. This arises from the fact that electrons with parallel spins experience a smaller repulsion than do those with opposed spins. Blake [16] showed that whether one chooses the familiar real orbitals, or imaginary ones with defined m_1 values, the exchange energy contributes about 70% of the half-filled break for p^n configurations and 75% for d^n configurations. In the case of f^n configurations, Newman's coulomb and exchange integrals [17] suggest that the contribution is over 80%. From $[Xe]4f^1$ to $[Xe]4f^7$, ionization destroys 0, 1, 2, 3, 4, 5 and 6 parallel spin interactions, progressively raising I_3. At europium therefore, the +2 oxidation state reaches a stability maximum because afterwards, at $[Xe]4f^8$, the new electron goes in with opposed spin. Its loss then destroys no parallel spin interactions, and the 0–6 pattern is repeated from $[Xe]4f^8$ to $[Xe]4f^{14}$ where a second stability maximum occurs at ytterbium(II). A more formal treatment includes an explanation of the 1/4- and 3/4-shell effects related to Hund's second rule [15].

1.2
A General Principle of Lanthanide Chemistry

Our analysis of thermodynamic stabilities has been developed through Eq. (3), but is of more general importance [18]. This is because it leads to a general principle composed of two parts. Each part deals with a particular class of reaction. The first class is typified by reaction 1. Because ligand field effects are very small, $L(MCl_2,s)$ and $L(MCl_3,s)$ change smoothly and slightly across the series, and the variations in $\Delta G^0(1)$ are completely dominated by those in I_3. This is apparent from the close parallelism between the two quantities. Under such cir-

cumstances, a change in the ligands leaves the irregularities largely unaffected, and the I_3-type variation in Fig. 1.1 is characteristic of *any* process in which the number of 4f electrons decreases by one.

The second class of reaction is that of processes in which the 4f electrons are conserved. The obvious examples are the complexing reactions of tripositive lanthanide ions. Here the irregularities due to changes in inter-electronic repulsion almost entirely disappear. We then get the slight smooth energy change whose consequences were so familiar to 19th century chemists, who struggled with the separation problem.

In many cases, lanthanide reactions can either be assigned exclusively to one of these two classes, or they show deviations that the classification makes understandable. In Fig. 1.2, we plot the values of ΔH^0 for the complexing of the tripositive aqueous ions by $EDTA^{4-}$(aq), a reaction in which the 4f electrons are conserved. The irregularities are negligible at the chosen scale. Also shown are the values of ΔH_f^0 (MCl_3,s) which refer to:

$$M(s) + 3/2Cl_2(g) = MCl_3(s) \qquad (6)$$

Here, for nearly all of the elements, the number of 4f electrons in the metallic state and in the trichloride is the same, so we expect a largely smooth energy

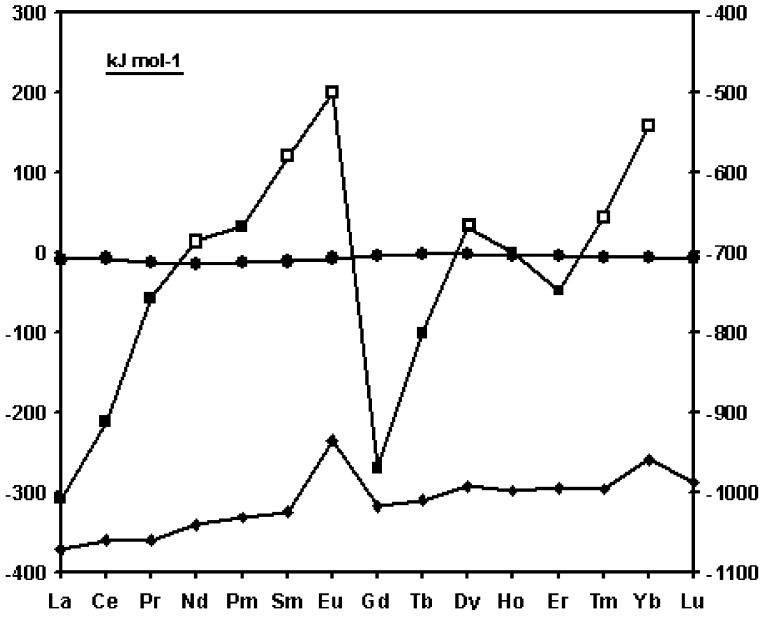

Fig. 1.2 Standard enthalpy changes of (a) the complexing of lanthanide ions in aqueous solution by $EDTA^{4-}$ (• left-hand axis); (b) the standard enthalpy change of reaction 2, the dichloride being a di-f compound (left-hand axis; ■ estimated value; □ experimental value); (c) the standard enthalpy change of reaction 6 (◆ right-hand axis). Data are from Refs. [11, 13, 14, 18 and 19].

variation. This is what we get. The exceptions are at europium and ytterbium, which form two-electron metals. In these two cases, reaction 6 is one in which the number of 4f electrons decreases by one. We can assume that the energy variation would be smooth if europium and ytterbium were three-electron metals like the other lanthanides. The observed deviations of about 85 and 40 kJ mol^{-1} then tell us the stabilizations that europium and ytterbium metals achieve by adopting a two- rather than a three-electron metallic state [9, 19]. Finally Fig. 1.2 contains the values of $\Delta H^0(2)$, the standard enthalpy of disproportionation of an alkaline earth-like dichloride. In nearly all cases, this is a process in which the number of 4f electrons decreases by one, and we see the extreme, but characteristic, I_3-type variation. Again the exceptions are at europium and ytterbium where the occurrence of two-electron metals on the right-hand side of the equation lowers the values by about 28 and 13 kJ mol^{-1}, respectively.

The principle introduced above is best exploited by classifying lanthanide compounds not by oxidation state, but by the number of 4f electrons at the metal site. For example, the reaction

$$\mathrm{MS(semi\text{-}conductor)} = \mathrm{MS(metallic)} \tag{7}$$

is one in which there is no change in *formal* oxidation state. In this sense, it resembles the EDTA complexing reaction of Fig. 1.2. But the energy variation is quite different. The reaction is one in which the 4f electron population decreases by one and its energy variation parallels I_3. Thus we observe semiconductors at Sm, Eu and Yb, and metallic sulfides at the other lanthanide elements. By using these ideas, quantitative values of $\Delta G^0(7)$ have been estimated [20]. If we label species which contain the same number of 4f electrons as the $[Xe]4f^{n+1}$configuration of the free M^{2+} ion, di-f, and those with the same number of 4f electrons as the $[Xe]4f^n$ configuration of the free M^{3+} ion, tri-f, then reaction 7 is one in which a di-f to tri-f transformation occurs and the number of 4f electrons decreases by one. This classification simplifies discussion of "lower oxidation states" of the lanthanide elements [2].

1.3 Extensions of the First Part of the Principle

The principle just outlined has two parts. The first part deals with redox processes and was developed here by examining the relative stabilities of the +2 and +3 oxidation states of the lanthanides. It can be extended in a variety of ways. Thus if the I_3 variation is shifted one element to the right, it tells us the nature of the I_4 variations, and accounts for the distribution of the +4 oxidation states of the lanthanides [2, 10, 15]. Their stability shows maxima at cerium(IV) and terbium(IV), decreasing rapidly as one moves from these elements across the series.

Similar principles apply to the actinides. The +2 oxidation state is present in dipositive aqueous ions and alkaline earth-like dihalides. In the first half of the

series only americium, where the Am^{2+} ion has the half-shell configuration $[Rn]5f^7$, forms such a dihalide. The drop in I_3 suppresses further dihalide formation at curium and berkelium, but such compounds reappear at californium and einsteinium. By mendeleevium, the dipositive aqueous ion is more stable than $Eu^{2+}(aq)$, and at nobelium, $No^{3+}(aq)$ is a stronger oxidizing agent than dichromate.

The +4 oxidation state is most stable at thorium, which lies beneath cerium. Its stability then decreases progressively until we reach curium where aqueous solutions containing the tetra-positive state must be complexed by ligands such as fluoride or phosphotungstate. Even then, they oxidize water and revert to curium(III). The expected drop in I_4 between curium and berkelium provides $Bk^{4+}(aq)$ with a stability similar to that of $Ce^{4+}(aq)$, but the decrease in stability is then renewed, and beyond californium, the +4 oxidation state has not yet been prepared [2, 10, 15].

In the lanthanide and actinide series, arguments like these are greatly eased by the very small ligand field effects. Consider the reaction

$$M^{2+}(aq) + H^+(aq) = M^{3+}(aq) + 1/2\,H_2(g) \tag{8}$$

The *variations* in ΔG^0 across the series are given by:

$$\Delta G^0(8) = I_3 - \Delta H_h^0(M^{2+}, g) + \Delta H_h^0(M^{3+}, g) + C \tag{9}$$

Here ΔH_h^0 (M^{n+},g) is the enthalpy of hydration of the gaseous M^{n+} ion, and the entropy change is assumed to be constant. Because ligand field effects are very small, the hydration enthalpies vary smoothly and slightly across the series, and the variations in $\Delta G^0(8)$ are dominated by those in I_3. If we move to the first transition series, the values of I_3 follow the expected pattern. They increase from Sc^{2+} to Mn^{2+} where we reach the half-shell configuration $[Ar]3d^5$, and then drop steeply at Fe^{2+}. The increase is then renewed up to the full shell at zinc. But the hydration enthalpies no longer vary smoothly. They show double-bowl shaped variations explained by octahedral ligand field stabilization energies. Because H_2O is a weak field ligand, the bowls are not too deep. The $\Delta G^0(8)$ variations are therefore still dominated by those in I_3, albeit in an attenuated form. Thus at the beginning of the series, Sc^{2+} (aq) and Ti^{2+} (aq) are unknown. V^{2+} (aq) and Cr^{2+} (aq) exist but are readily oxidized by air, and Mn^{2+} (aq) is stable with respect to this reaction. The decrease in stability of the dipositive oxidation state between manganese and iron is neatly shown by the ready occurrence of the reaction

$$Mn^{3+}(aq) + Fe^{2+}(aq) = Mn^{2+}(aq) + Fe^{3+}(aq) \tag{10}$$

After iron, the tripositive ions are unstable: $Co^{3+}(aq)$ slowly oxidizes water at room temperature, and $Ni^{3+}(aq)$, Cu^{3+} (aq) and $Zn^{3+}(aq)$ do not exist [15, 33].

1.4 Extensions of the Second Part of the Principle

As Fig. 1.2 shows, thermodynamics distinguishes lanthanide reactions in which the 4f population changes from those in which the 4f population is conserved. In the latter type of reaction, the second part of our principle states that the energy variation is nearly smooth. Why do we need the qualification "nearly"? First, there are many important chemical changes to which thermodynamics is rather insensitive. Structure is often a good example. The smooth energy variation in Fig. 1.2 refers to a complexing reaction in aqueous solution. It is generally accepted that, as we move across the lanthanide series, the coordination number of the aqueous ion changes. Yet on the scale of Fig. 1.2, this produces no obvious irregularities. A more relevant structural case is that of the lower halides of La, Ce, Pr and Gd [21, 22]. These are elements which do not form di-f alkaline earth-like dihalides, and their lower halides contain significant metal–metal bonding. Again, the work was both pioneered and continued by Corbett [3]. In such compounds, the 4f populations at the metal sites seem to be identical with those in both the metallic element and the trihalide. Thus stability is determined by reactions such as

$$Gd_2Cl_3(s) = Gd(s) + GdCl_3(s) \tag{11}$$

in which all substances are tri-f and there is no change in the 4f electron populations. With three bonding electrons per metal atom, there are six such electrons on each side of Eq. (11). Three can be allocated to the formation of bonds with chlorine, and three to the formation of multi-centred Gd–Gd bonding. So the bonding on each side of the equation is similar: on the left it is distributed over one substance; on the right over two. If correct, this suggests that $\Delta H^0(11)$ should be close to zero and, in fact, the value is only 30±15 kJ mol^{-1} [23]. An important contribution to the small positive value seems to be the splitting of the 5d bands generating the metal–metal interaction in Gd_2Cl_3. This stabilizes the compound and makes it a semiconductor [24].

Unlike the di-f dihalides, such compounds differ little in energy from both the equivalent quantity of metal and trihalide, and from other combinations with a similar distribution of metal–metal and metal–halide bonding. So the reduced halide chemistry of the five elements shows considerable variety, and thermodynamics is ill-equipped to account for it. All four elements form di-iodides with strong metal–metal interaction, PrI_2 occurring in five different crystalline forms. Lanthanum yields LaI, and for La, Ce and Pr there are halides M_2X_5 where X = Br or I. The rich variety of the chemistry of these tri-f compounds is greatly increased by the incorporation of other elements that occupy interstitial positions in the lanthanide metal clusters [3b, 21, 22].

These difficulties show that the description "nearly smooth" for the energies of inter-conversion of tri-f compounds is a confession of inadequacy. But other kinds of reaction in which the 4f electrons are conserved suggest that it may be possible to refine "nearly smooth" into something more precise. To this we now turn.

1.5
The Tetrad Effect

What became known as the tetrad effect was first observed in the late 1960s during lanthanide separation experiments [25]. Fig. 1.3 shows a plot of log K_d, where K_d is the distribution ratio between the aqueous and organic phases in a liquid–liquid extraction system. There are four humps separated by three minima, first at the f^3/f^4 pair, secondly at the f^7 point, and thirdly at the f^{10}/f^{11} pair. Calls for an explanation were answered by Jorgensen and elaborated by Nugent [26]. When a lanthanide ion moves from the aqueous to the organic phase, the nephelauxetic effect leads to a small decrease in inter-electronic repulsion within the 4f shell. This decrease varies irregularly with atomic number and is responsible for the irregularities in Fig. 1.3.

This initial explanation and subsequent developments use Jorgensen's refined spin-pairing energy theory. This theory refers the repulsion energy changes to a baseline drawn through points at the f^0, f^1, f^{13} and f^{14} configurations. But, for reasons that will become apparent, I shall use a baseline through the f^0, f^7 and f^{14} points. Column 2 of Table 1.2 repeats the formulae for $E_{rep}(f^n)$ taken from Table 1.1. The baseline function g(n) in column 3 passes smoothly through the f^0, f^7 and f^{14} values and takes the form

$$g(n) = 1/2\,n(n-1)E^0 + (9\,n/14)(n-7)E^1 \qquad (12)$$

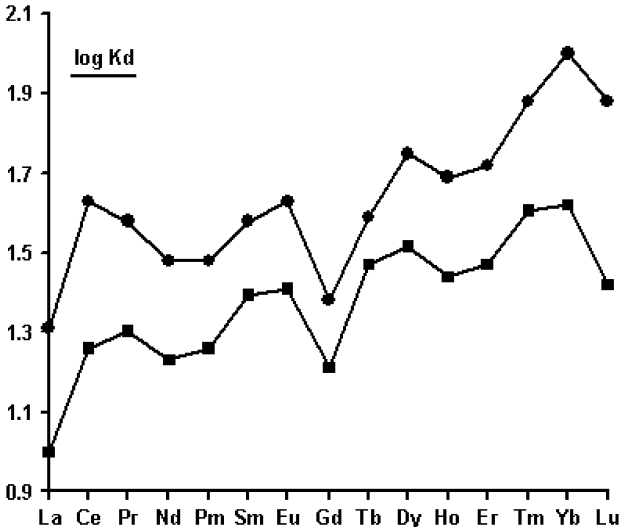

Fig. 1.3 (a) Observed values of log K_d where K_d is the distribution constant for lanthanide ions between aqueous 11.4 M LiBr in 0.5 M HBr and 0.6 M $(ClCH_2)PO(OC_8H_{17})_2$ in benzene (Ref. [26a]; upper plot). (b) A similar variation constructed by using the theory of Table 1.2 (lower plot; see text).

Column 4 is the difference between columns 2 and 3. It tells us the deviations of the total 4f inter-electronic repulsion energy from the f^0, f^7 and f^{14} baseline. In between f^0 and f^7, and again between f^7 and f^{14}, the relative sizes of E^1 and E^3 are such that the repulsion is raised. In discussing the effect upon *reactions*, the quantities E^1 and E^3 should be replaced by ΔE^1 and ΔE^3. If ΔE^1 and ΔE^3 are both negative, then the formulae of column 4 can reproduce the form of the log K_d variation. The change in ΔE^1 increases the $f^1 - f^6$ and $f^8 - f^{13}$ values relative to those at f^0, f^7 and f^{14}, but that in ΔE^3 moderates those increases, most notably at f^3, f^4, f^{10} and f^{11}. This can reproduce the four-hump variation of Fig. 1.3. The lower plot has been constructed by superimposing the formulae in column 4 of Table 1.2, with the values $\Delta E^1 = -28$ cm^{-1} and $\Delta E^3 = -7$ cm^{-1}, upon a linear increase of 0.03 per element. The parallelism is obvious. Effects of this sort are of interest to geochemists. Tetrad patterns in the concentrations of lanthanide elements have been used to explore the evolutionary history of igneous rocks such as granites [27]. The effect has also been invoked to explain the distribution of rare earth elements in sea water [28].

Very often, the tetrad effect is *not* clearly discernible in the energies of processes in which 4f electrons are conserved. It may, for example, be obscured by irregularities caused by structural variations in either reactants or products. This is especially likely given the willingness of lanthanide ions to adopt a variety of coordination geometries. There is, however, no doubt that tetrad-like patterns are often observed. But does Table 1.2 provide a convincing explanation of what is seen?

Imagine a thoroughly convincing test of the explanation. We begin with a reaction in which the 4f electrons are conserved. In the sequence La → Lu, each

Table 1.2 The excess inter-electronic repulsion for f^n configurations (column 4), relative to a smoothly varying baseline function, $g(n)$, drawn through the formulae for f^0, f^7 and f^{14}.

n	$E_{rep}(f^n)$	g (n)	$[E_{rep}(f^n) - g(n)]$
0	0	0	0
1	0	$-(54/14)E^1$	$(54/14)E^1$
2	E^0-9E^3	$E^0-(90/14)E^1$	$(90/14)E^1-9E^3$
3	$3E^0-21E^3$	$3E^0-(108/14)E^1$	$(108/14)E^1-21E^3$
4	$6E^0-21E^3$	$6E^0-(108/14)E^1$	$(108/14)E^1-21E^3$
5	$10E^0-9E^3$	$10E^0-(90/14)E^1$	$(90/14)E^1-9E^3$
6	$15E^0$	$15E^0-(54/14)E^1$	$(54/14)E^1$
7	$21E^0$	$21E^0$	0
8	$28E^0+9E^1$	$28E^0+(72/14)E^1$	$(54/14)E^1$
9	$36E^0+18E^1-9E^3$	$36E^0+(162/14)E^1$	$(90/14)E^1-9E^3$
10	$45E^0+27E^1-21E^3$	$45E^0+(270/14)E^1$	$(108/14)E^1-21E^3$
11	$55E^0+36E^1-21E^3$	$55E^0+(396/14)E^1$	$(108/14)E^1-21E^3$
12	$66E^0+45E^1-9E^3$	$66E^0+(540/14)E^1$	$(90/14)E^1-9E^3$
13	$78E^0+54E^1$	$78E^0+(702/14)E^1$	$(54/14)E^1$
14	$91E^0+63E^1$	$91E^0+(882/14)E^1$	0

reactant must be isostructural, as must each product. Uncertainties in the energy variation for the reaction must be smaller than the irregularities attributed to the tetrad effect. Finally, the spectra of each reactant and product must be analyzed to provide values of ΔE^1 and ΔE^3, and the auxiliary changes in ligand field stabilization and spin-orbit coupling energies. The size of the humps can then be evaluated, auxiliary contributions subtracted and the residues compared with the values predicted using the values of ΔE^1 and ΔE^3. Published tests are impressive, but fall short of this standard [29]. The difficulty is the small size of lanthanide nephelauxetic effects compared with uncertainties in the input data.

1.6 The Diad Effect

Quantitative tests of the effect of inter-electronic repulsion on the energies of reactions in which 4f electrons are conserved are therefore very difficult. But they are possible for reactions in which 3d electrons are conserved, and the standards of proof set out in the previous section can then be applied. In the first transition series, variations in lattice and hydration enthalpies take the form of double-bowl shapes. Standard texts have long attributed these irregularities to what George and McClure called inner-orbital splitting [30]. This splitting is induced by the symmetry of the ligand field. George and McClure noted that in some cases, especially the hydration enthalpies of the M^{3+} ions, the size of the bowls was too large to be consistent with spectroscopic values of the orbital splitting parameter Δ. They thought that the discrepancy might be explained by changes in the spin-orbit coupling energy, or by a relaxation energy that allows for the effect of changes in bond length induced by the ligand field. These additional terms, however, only increased the disagreement. In the 1990s, the discrepancy was attributed to the nephelauxetic effect, using an explanation of the kind embodied in Table 1.2 [31].

In d^n series, we use a d^0, d^5 and d^{10} baseline, and the values analogous to those given in column 3 of Table 1.2 are expressed in terms of the Racah parameters B and C. At d^1, d^4, d^6 and d^9, the values are $(7B+2.8C)$; at d^2, d^3, d^7 and d^8, they are $(6B+4.2C)$. When a gaseous ion becomes coordinated, the nephelauxetic effect ensures that ΔB and ΔC are both negative. The relative sizes of ΔB and ΔC are such as to give rise to a bowl-shaped contribution to the binding energy in each half of the series. So, whereas in the lanthanide series there was a tetrad effect, here we have a *diad* effect that supplements the orbital stabilization energies of the ligand field. In the first transition series, the method recommended in the previous section has been applied to the lattice enthalpies of K_3MF_6 [31], MF_2, MCl_2 and MI_2 [32], and to the hydration enthalpies of M^{2+} and M^{3+} [33, 34]. The four contributions to the irregularities were calculated. These are the orbital stabilization energies, ΔE_{os}, the irregularities due to the nephelauxetic effect, ΔE_{rep}(irreg), spin-orbit coupling, ΔE_{so}, and the relaxation energy, ΔE_{rlx}. Along the chosen baseline, these four quantities are all zero and this is its main advantage.

Table 1.3 Estimated values of the four components of the contribution made by ligand field stabilization energy to the lattice enthalpy of K_3CuF_6, to the hydration enthalpy of $Ni^{2+}(aq)$, $\Delta H_h^0(Ni^{2+},g)$, and to the standard enthalpy change of reaction 13.

	ΔE_{os}	ΔE_{rep}(irreg)	ΔE_{so}	ΔE_{rlx}	Total
			kJ mol^{-1}		
$L(K_3CuF_6)$	–202	–156	+16	+14	–328
$\Delta H_h^0(Ni^{2+}, g)$	–123	–18	+12	+10	–119
ΔH^0(13)	+0.3	–3.3	+0.8	0	–2.2

Table 1.3 contains values for two $3d^8$ cases. At K_3CuF_6, ΔE_{rep}(irreg) contributes about 40% of the total stabilization, but at $Ni^{2+}(aq)$ only 15%. This is because in the first transition series, the nephelauxetic effect increases substantially when the oxidation state increases from +2 to +3. The relatively small contribution for the $M^{2+}(aq)$ ion explains why text books use this example to explain the double bowl shapes: ΔE_{rep}(irreg) is almost exactly cancelled by the sum of ΔE_{so} and ΔE_{rlx}, so the total stabilization is nearly equal to the orbital stabilization energy. In most other cases, ΔE_{rep}(irreg) is much more important and may play an important role in sustaining the Irving-Williams rule in complexing reactions [32, 33].

In the lanthanide series, the equivalent values are much reduced by the retreat of the 4f electrons into the xenon core. This is so whether we consider processes that involve the condensation of gaseous ions, or conventional reactions. Table 1.3 includes data for the change

$$NdF_3(s) + 3/4\,O_2(g) = 1/2\,Nd_2O_3(s) + 3/2\,F_2(g) \qquad (13)$$

These have been calculated from Caro's spectroscopic analyses [35]. The ligands come from opposite ends of the nephelauxetic series, so for a lanthanide reaction, ΔE_{rep}(irreg) should be relatively large. Even so, although it proves to be the largest contributor to the overall change, ΔE_{os} and ΔE_{so} are significant. Quantitative analyses of claimed examples of the tetrad effect must take such terms into account.

It is striking that, despite its small size, the tetrad effect was discovered before the diad effect. This is because the diad effect occurs in d-electron systems and is therefore masked by the orbital stabilization energies produced by the stronger ligand field.

References

1 Jantsch, G.; Klemm, W. *Z. Anorg. Allg. Chem.*, **1933**, *216*, 80.
2 Johnson, D.A. *Advan. Inorg. Chem. Radiochem.* **1977**, *20*, 1.
3 Corbett, J.D. (a) *Rev. Chim. Miner.* **1973**, *10*, 239; (b) *J. Chem. Soc. Dalton Trans.* **1996**, 575.
4 Corbett, J.D.; McCollum, B.C.; *Inorg. Chem.* **1966**, *5*, 938.
5 Johnson, D.A.; Corbett, J.D. *Colloq. Int. CNRS* **1970**, *180*, 429.
6 Caro, P.E.; Corbett, J.D. *J. Less-Common Met.* **1969**, *18*, 1.
7 Corbett, J.D.; Pollard, D.L.; Mee, J.E. *Inorg. Chem.* **1966**, *5*, 761.
8 Evans, W.J.; Zucchi, G.; Ziller, J.W. *J. Amer. Chem. Soc.* **2003**, *125*, 10.
9 Johnson, D.A. *J. Chem. Soc. A* **1969**, 1525.
10 Johnson, D.A. *J. Chem. Soc. A* **1969**, 1529.
11 Johnson, D.A. *J. Chem. Soc. A* **1969**, 2578.
12 *http://physics.nist.gov/PhysRefData/ASD/levels*; see also Spector, N.; Sugar, J.; Wyart, J.F. *J. Opt. Soc. Am. B* **1997**, *14*, 511.
13 Morss, L.R. *Standard Potentials in Aqueous Solution* (Bard, A.J.; Parsons, R.; Jordan, J. eds.); Marcel Dekker, New York, 1985; p. 587.
14 Cordfunke, E.H.P.; Konings, R.J.M. *Thermochim. Acta* **2001**, *375*, 17.
15 Johnson, D.A. *Some Thermodynamic Aspects of Inorganic Chemistry*, 2nd ed; Cambridge University Press, 1982; Chapter 6 and problems 6.6–6.9.
16 Blake, A.B. *J. Chem. Educ.* **1981**, *58*, 393.
17 Newman, J.B. *J. Chem. Phys.* **1967**, *47*, 85.
18 Johnson, D.A. *J. Chem. Educ.* **1980**, *57*, 475.
19 Johnson, D.A. *J. Chem. Soc. Dalton Trans.* **1974**, 1671.
20 Johnson, D.A. *J. Chem. Soc. Dalton Trans.* **1982**, 2269.
21 Meyer, G. *Chem. Rev.* **1988**, *88*, 93.
22 Meyer, G.; Wickleder, M.S. *Handbook on the Physics and Chemistry of the Rare Earths* (Gschneidner, K.A.; Eyring, L. eds.), North Holland, Amsterdam, **2000**, *28*, 53.
23 Morss, L.R.; Mattausch, H.; Kremer, R.; Simon, A.; Corbett, J.D. *Inorg. Chim. Acta* **1987**, *140*, 107.
24 Bullett, D.W.; *Inorg. Chem.* **1985**, *24*, 3319.
25 Peppard, D.F.; Mason, G.W.; Lewey, S. *J. Inorg. Nucl. Chem.* **1969**, *31*, 2271.
26 (a) Peppard, D.F.; Bloomquist, C.A.; Horowitz, E.P.; Lewey, S.; Mason, G.W. *J. Inorg. Nucl. Chem.* **1970**, *32*, 339. (b) Jorgensen, C.K. *ibid.*, 3127. (c) Nugent, L.J. *ibid.*, 3485.
27 Veksler, I.V.; Dorfman, A.M.; Kamenetsky, M.; Dulski, P.; Dingwell, D.B. *Geochem. Cosmochim. Acta* **2005**, *69*, 2847.
28 Kawabe, I.; Toriumi, T.; Ohta, A.; Miura, N. *Geochem. J.* **1998**, *32*, 213.
29 Kawabe, I. *Geochem. J.* **1992**, *26*, 309.
30 George, P.; McClure, D.S. *Prog. Inorg. Chem.* **1959**, *1*, 381.
31 Johnson, D.A.; Nelson, P.G. *Inorg. Chem.* **1995**, *34*, 3253.
32 Johnson, D.A.; Nelson, P.G. *J. Chem. Soc. Dalton Trans.* **1995**, 3483.
33 Johnson, D.A.; Nelson, P.G. *Inorg. Chem.* **1995**, *34*, 5666.
34 Johnson, D.A.; Nelson, P.G. *Inorg. Chem.* **1999**, *38*, 4949.
35 (a) Caro, P.; Derouet, J.; Beaury, L.; Soulie, E. *J. Chem. Phys.* **1979**, *70*, 2542. (b) Caro, P.; Derouet, J.; Beaury, L.; Teste de Sagey, G.; Chaminade, J.P.; Aride, J.; Pouchard, M. *J. Chem. Phys.* **1981**, *74*, 2698.